Design status of ITER ECH upper launcher mirrors

F. Sanchez, R. Bertizzolo, R. Chavan, A. Collazos, J. Duron, M.A.Henderson, J.D. Landis, H. Shidara.
CRPP-EURATOM, Confederation Suisse, EPFL, CH-1015 Lausanne Switzerland

***Abstract*— The ITER ECH upper launcher is devoted to directing up to 8 2MW beams per port plug over half of the plasma cross section. A focusing mirror is used to achieve a very narrow deposition profile to stabilize MHD activity such as the neoclassical tearing modes (NTMs) and the sawtooth oscillation. The beam deposition location is changed via a steering mirror with up to +/-7 deg (+/-14 deg beam), which allows access from inside mid radius out to nearly the plasma edge. The steering mechanism uses a frictionless backlash free system to avoid sticking, thus increasing the reliability.**

A small percentage (<0.5%) of the beam is absorbed upon each reflection from the mirror surface, resulting in absorbed peak power densities ranging from ~2.0MW/m^2 (focusing and steering mirrors) to 3.6MW/m^2 (waveguide mitre bend mirror). The cooling of each mirror has been analysed under ITER conditions using theoretical and finite element modeling (using ANSYS and ANSYSWORKBENCH).

The design optimization of the steering mirror has been given considerable attention, aiming at lowering the peak heat load density, while limiting the induced current from the incident changing magnetic field that occurs during a plasma disruption event.

The analysis of the mitre bend mirror has been compared to experimental data taken from long pulse (up to 1'000s) , high power (0.3 to 0.8MW) operation, which has been performed in collaboration with with JAEA, GA, CNR, EFDA and CRPP to validate the FE results and to demonstrate that it can withstand high power densities arising from up to 2MW incident power.

This paper will overview the current design status along with the critical design issues for the different in-launcher mirrors.

I. INTRODUCTION

The ITER ECRH upper port antenna (or launcher) will be used to drive current locally for stabilising the neoclassical tearing mode (NTM) by depositing current inside of the island which forms on the q=3/2 or 2 rational magnetic flux surfaces and control the sawtooth instability by driving current near the q=1 surface. This requires the launcher to be capable of steering the focused beam deposition location across the resonant flux surface over the range where the q=1, 3/2 and 2 surfaces are expected to be found (roughly the outer half of the plasma). A two mirror system (1 focusing-fixed and 1 flat-steering) for focusing and redirecting the beam towards the q=3/2 or 2 flux surfaces for all envisioned plasma equilibria is used.

A simplified poloidal section view of the current FS launcher design is shown in figure 1. Eight circular waveguides enter at the port entrance on the right, with the waveguides arranged in two rows of four. A miter bend `dog-leg' assembly is used to angle the 8 beams (both in toroidal and poloidal directions) to one single focusing mirror, the incident beams partially overlap in both toroidal and poloidal directions. The reflected beams are then directed downward to two separate flat steering mirrors, which redirect the beams into the plasma with a toroidal injection angle. Since the beams are allowed to expand from the waveguide aperture, they can be refocused to a narrow waist far into the plasma (>1.6m after steering mirror). The angular rotation of the steering mirror (±6.5˚) provides access along the resonance layer from Z_{res} = 1.8 to 3.6m

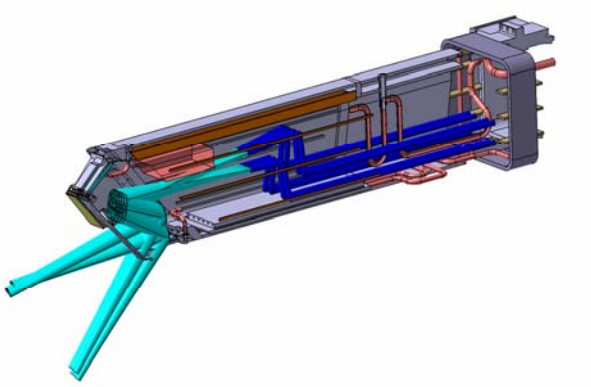

Figure 1. mm-wave components in the upper port

II. THE STEERING MECHANISM

The steering mechanism providing the rotation uses a frictionless and backlash free mechanical system based on the compliant deformation of structural components to avoid the in-vessel tribological difficulties. Traditional designs are based on push-pull rods acting on a mirror which rotate with ball bearings, they present the risk of gripping or result in stick-slip movements. The ball bearings are replaced with a set of flexure pivots while the classic actuation through push&pull rod is replaced by a pneumatic system consisting on a fast feed line, bellows and springs, in which the pressure acting on the bellows pushes the mirror against the compressive spring. The rotation of the mirror is thus produced by the counteraction between the forces exerced by the springs and the bellows, themselves piloted by the pressure of the system. A servovalve placed outside of the port plug and connected to the bellows by a small tube will control this pressure. The system also incudes flexible cooling pipes which allow the water feeding of the rotating mirror

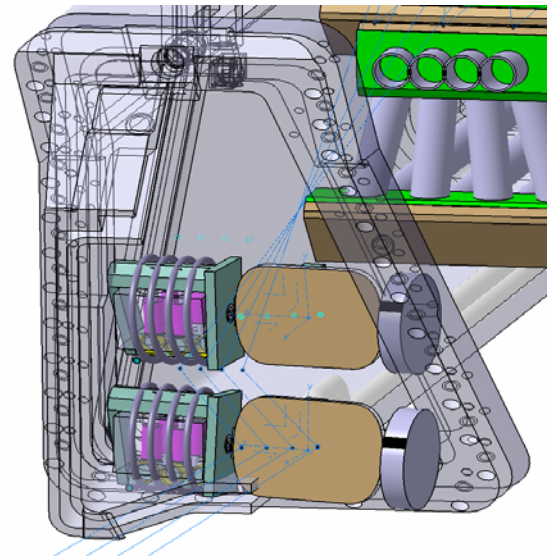

Figure 2. The front steering mechanisms at the front of the upper port plug.

III. THE FRONT STEERING MIRROR

The mirror dimensions are 290mm (toroidal) x 210mm (poloidal). It is made in two layers: a reflective surface made from copper, and a high resistive layer made in SS-316-L(N) to provide structural rigidity to the mirror. Electrical insulation breaks could be further introduced on the back side limiting the effective thickness.

The spot sizes on both the focusing and steering mirrors are relatively large (65.0mm and ~50.0mm respectively) and, as a result, the peak power density is reduced significantly despite the partial overlap of multiple 2.0MW beams. The maximum power density reaches ~2MW/m^2, which occurs on the lower steering mirror. Absorbed power is calculated assuming circular polarization and an absorption coefficient of 0.005 to account for increased temperature, surface roughness and surface impurity effects.

The EM forces related to the induced currents during a disruption were estimated for the steering mirror in the worst configuration and assuming no shielding effect from the port wall, dB_P/dt=25T/s (plasma current 17.85MA and linear current decay time 0.04s [11]) and B_T=5.0T. The latest values given for disruptions of type II and III [12] were accounted for the final design of the mirror.

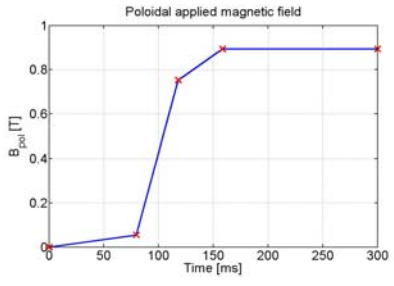

Figure 3. Time varying poloidal field from a VDE III

Identify applicable sponsor/s here. *(sponsors)*

A. THERMOMECHANICAL ANALYSIS

To provide a parametric approach, the variants were created in DESIGNMODELLER (from ANSYS WORKBENCH) and the thermal-mechanical analysis were first performed.

The design criteria adopted for these analysis were:

- Maximum temperature on the mirror surface should be below 300 C
- Maximum temperature on the inner channel of water 240 C (limited by the water boiling point at 3 MPa)
- Minimum radius of curvature due to mirror bending 10m
- Avoid thermal runaway due to neutronic heating (evacuated by radiation) in the case of a coolant loss (non actively cooled mirror)
- Film coefficient below 60.000 W/m^{2}K

Two thermal loads occur on the front steering mirror: neutronic heating (1 MW/m^3) and the mm-wave imput beams (4 beams per mirror).

The ohmic loss of a single incident mm-wave beam is described by the gaussian heat flux distribution :

$$\frac{dP}{dA} = \frac{P_0 \, \eta_{abs} \, s}{\pi \, w_m^{\,2}} \left[1 + \cos^2(\theta_{inc}) \right]$$

Where $\mathbf{P_0}$: input power (2 MW) ,

$\boldsymbol{\omega_m}$: beam spot size on mirror

$\boldsymbol{\theta_{inc}}$: beam incidence angle to mirror surface normal

s: surface roughness factor (2)

$\boldsymbol{\eta_{abs}}$: RF absorption factor

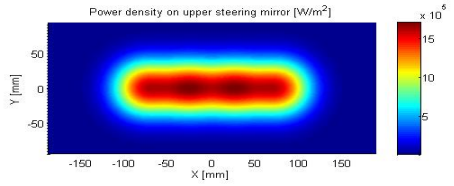

Figure 4. Heat load on the mirror (4 incident mm-wave beams)

Different configurations were analysed and In order to minimise beam alteration effects due to mirror deformation, the thermal gradients may be reduced with the integration of a non uniform cooling channel spacing pattern, while limiting the peak temperature in the center region of the mirror.

The back plate (beam-like support structure) provides rigidity to the mirror while minimising the closed loop paths.

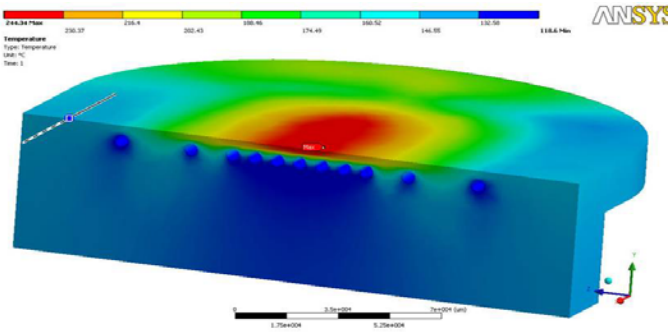

Figure 5. Temperature distribution on the mirror

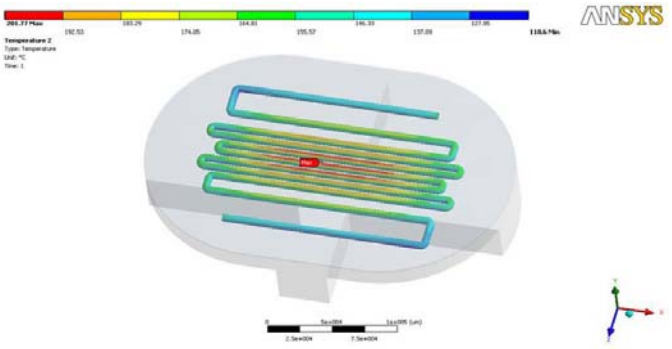

Figure 6. Wall temperature of the non-uniformly spaced cooling channels

With this configuration, the mirror bends outward by 0.2mm resulting in a radius of curvature equivalent to 49m, having a negligible effect on the beam defocusing.

B. ELECTROMAGNETIC ANALYSIS

The steering mirror is simultaneously exposed to a constant toroidal field and a time varying poloidal field. (During a plasma disruption event, the plasma current (up to 17MA) is quenched rapidly, (~40ms) resulting in a large changing magnetic field of the order of 25T/s in the vicinity of the steering mirror.

These fields induce currents with the magnitude depending on the size of the conductive loops established on the mirror body, and thus a net torque is generated on the mirror. The torque is perpendicular to the mirror surface, and results in a force on the flexure pivots and a rotation of the steering mirror. In this way, the steering mirror has an impact on the steering mechanism design and the size of the overall assembly.

ANSYS WORKBENCH 11 doesn't allow transient electromagnetic analysis. ANSYS can deal with it, but the loads are based on an edge simulation and thus, the FE formulation of ANSYS (SOLID117) doesn't allow to impose the combined poloidal (constant) and toroidal (time-varying) 3-D B(t), so a laboratory technique was applied for getting a fairly uniform magnetic field : the helmholtz coils setup.

A Helmholtz pair consists of two identical circular magnetic coils that are placed symmetrically one on each side of the experimental area along a common axis, and separated by a distance equal to the radius of the coil. Actually, a slightly larger separation improves the field uniformity. Each coil carries an equal electrical current flowing in the same direction. A cylindrical region extending between the centers of the two coils and approximately 1/5 of their diameter will have a nearly spatially uniform magnetic field.

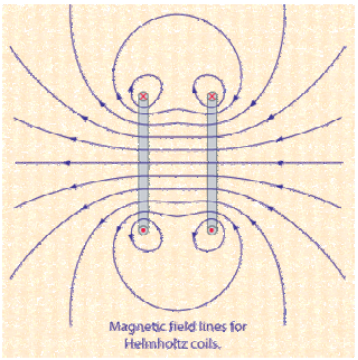

Figure 7. Magnetic field lines for Helmoltz coils.

With the constrain imposed by the SOLID117 edge element formulation is solved: only the toroidal field is applied as a real magnetic field, while the poloidal field is generated by the time-varying currents applied on the coils. In order to validate the method and the meshing size, a probe to estimate the value of the field in the central region of the coils was settled, and a constant current was injected in the coils,indicating a field value of 1.053T, in good agreement with theory (1.06T)

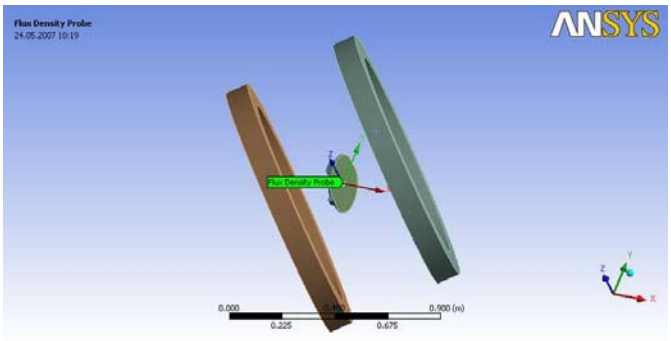

Figure 8. ANSYS set-up & flux probe.

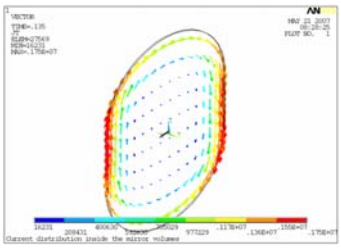

Figure 9. Induced currents in the mirror surface

The resulting induced torque on the mirror is ~1000Nm, resulting in a force of ~3 kN per flexure pivot (a flexure pivot is positioned on each side of steering mirror).

IV. THE MITRE BEND MIRROR

The mitre bend has the highest incident power density (Gaussian beam with a peak around 3.6MW/m^2) in both the ITER equatorial and upper port launchers (assuming 2MW/line).

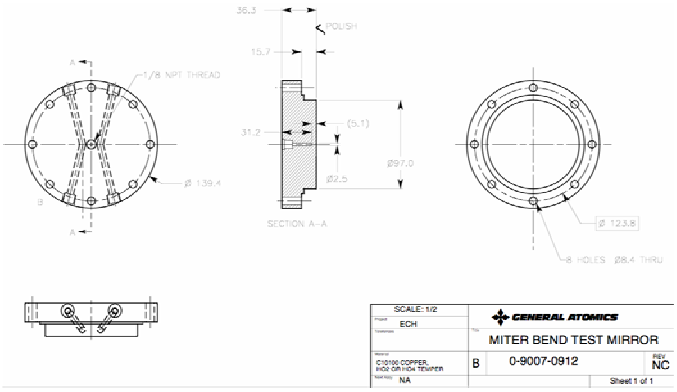

Figure 10. Geometry of the miterbend mirror

Normally, the HE_{11} mitre bend mirror is made of copper with a resistivity of the order of $1.72*10^{-6}\mu\Omega$-cm at 20ºC. The resistivity increases by ~40% in increasing the temperature from 20ºC to 120ºC (maximum inlet coolant temperature of the blanket cooling water), which corresponds to an 18% increase in absorption. In order to simulate the equivalent absorption from 2MW but using a 1MW source, then the absorption would have to be a factor of 2.36 larger (2*1.18). Such an increase in absorption can be achieved by increasing the surface resistivity by a factor of 5.57 (2.36^2) or ~$9.6*10^{-6}\mu\Omega$-cm. This has been made coating the copper mirror with a thin layer of nickel (7.5 to $11.5*10^{-6}\mu\Omega$-cm). The resistivity of the nickel-plated surface is ~$8.6*10^{-6}\mu\Omega$-cm., and surface roughness effects at millimetre-wave frequencies make the effective resistivity somewhat higher. This option maintains the same thermal conductivity since the thin nickel layer will have a negligible effect.

A FE model of the mitre bend mirror has been made using ANSYS as shown in figure 10 The size of the elements on the surface are of the order of 2mm, larger elements are used on the mirror back side to reduce calculation time. The model is used to estimate the thermal time constants, peak temperatures, mirror deformations and stress at three power levels (0.4, 0.7 and 1.0 MW) for the two mirrors (Cu and Ni coated). [1]

A simplified test of the mitre bend has been done in participation with JAEA, GA, CNR, EFDA and CRPP to demonstrate that the mitre bend can function with such power densities.

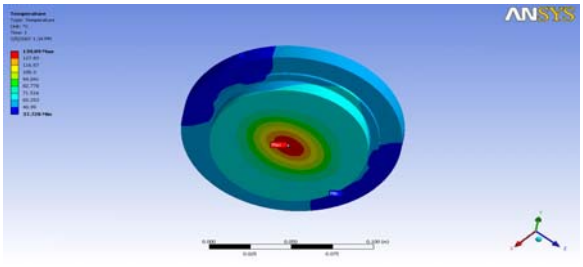

Figure 11. Temperature distribution on the mitre bend mirror

The figure 12 shows the lay-out used for these tests: the beam from the gyrotron passes straight through the switch and then through the mitre bend dogleg to the load. The first mitre bend housed the copper or nickel coated mirror, the second mitre bend being a control mitre bend.

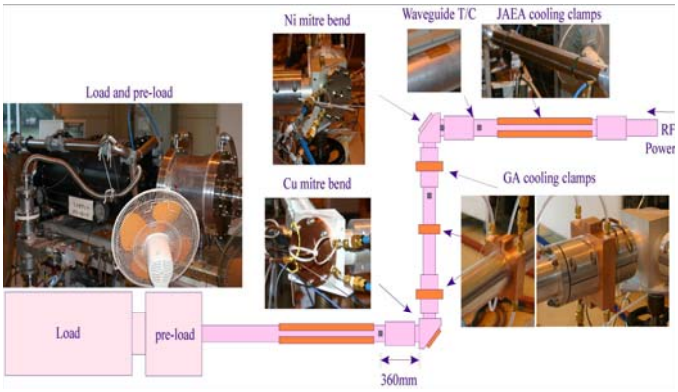

Figure 12. Layout of the JAEA test line in the region of the mitre bends.

V. CONCLUSIONS

ANSYS environment, although not specially developed for transient electromagnetic analysis, allows a multidisciplinary approach and show that the current design withstands the different load scenarios. At the current moment, the upper launcher mirrors are compatible with the different heat and electromagnetic loads due to the ITER environment. The maximum incident power (3.6 MW/m2) is reached in the mitre bend mirror, while the higher electromagnetic loads are supported by the front steering mirror.

ACKNOWLEDGMENT

The author would like to thank J. Duron for the Helmholtz coil approach and the comparison made between ANSYS and FLUX3D electromagnetic code.

This work was supported by the Swiss National Science Foundation. This work, supported by the European Communities under the contract of Association between EURATOM/ CRPP-EPFL, was carried out within the framework of the European Fusion Development Agreement. The views and opinions expressed herein do not necessarily reflect those of the European Commission.